



## Measurement of the $W$ Boson Helicity in Top Quark Decay at DØ

The DØ Collaboration

URL: <http://www-d0.fnal.gov>

(Dated: March 20, 2006)

We present a measurement of the fraction  $f_+$  of right-handed  $W$  bosons produced in top quark decays, based on a candidate sample of  $t\bar{t}$  events in the lepton+jets and dilepton decay modes. These data correspond to an integrated luminosity of  $370 \text{ pb}^{-1}$ , collected by the DØ detector at the Fermilab Tevatron  $p\bar{p}$  Collider at  $\sqrt{s} = 1.96 \text{ TeV}$ . We reconstruct the kinematics of the  $t\bar{t}$  and decay products, which allows for the measurement of the leptonic decay angle  $\theta^*$  for each event. By comparing the  $\cos\theta^*$  distribution from the data with those for the expected background and signal for various values of  $f_+$ , we find  $f_+ = 0.08 \pm 0.08(\text{stat}) \pm 0.05(\text{syst})$ . This measurement is consistent with the standard model prediction of  $f_+ = 3.6 \times 10^{-4}$ .

*Preliminary Results for Winter 2006 Conferences*

The top quark is by far the heaviest of the known fermions and is the only one that has a Yukawa coupling of order unity to the Higgs boson in the standard model. We search for evidence of new physics in the  $t \rightarrow Wb$  decay by measuring the helicity of the  $W$  boson. In the standard model, the top quark decays via the  $V - A$  charged current interaction, and almost always to a  $W$  boson and  $b$  quark. The  $W$  bosons produced from these decays are predominantly in either a longitudinal or a left-handed helicity state with fractions  $f_0$  and  $f_-$ , respectively. For any linear combination of  $V$  and  $A$  currents at the  $t \rightarrow Wb$  vertex [1],

$$f_0 \approx \frac{m_t^2}{2M_W^2 + m_t^2 + m_b^2} = 0.703 \pm 0.012 \quad (1)$$

where  $m_t$  is the mass of the top quark for which we use  $175 \pm 5$  GeV (consistent with the world average [2]),  $M_W$  is the mass of the  $W$  boson, and  $m_b$  is the mass of the bottom quark [2].

In this analysis, we fix  $f_0$  at 0.70 and measure the positive helicity fraction  $f_+$ . In the standard model,  $f_+$  is suppressed by a factor of  $(m_b/m_t)^2$  and is predicted at next-to-leading order to be  $3.6 \times 10^{-4}$  [3]. A measurement of  $f_+$  that differs significantly from this value would be an unambiguous indication of new physics. For example, an  $f_+$  value of 0.30 would indicate a purely  $V + A$  charged current interaction. A possible theoretical model that includes a  $V + A$  contribution at the  $t \rightarrow Wb$  vertex is an  $SU(2)_L \times SU(2)_R \times U_Y(1)$  extension of the standard model [4].

Measurements of the  $b \rightarrow s\gamma$  decay rate have indirectly limited the  $V + A$  contribution in top quark decays to less than a few percent [5]. However, direct measurements of the  $V + A$  contribution are still necessary because the limit from  $b \rightarrow s\gamma$  assumes that the electroweak penguin contribution is dominant. Direct measurements of the longitudinal fraction found  $f_0 = 0.91 \pm 0.39$  [6] and  $f_0 = 0.56 \pm 0.31$  [7]. Recent direct measurements of  $f_+$  have set limits of  $f_+ < 0.18$  [8],  $f_+ < 0.24$  [9] and  $f_+ < 0.25$  [10] at the 95% C.L.. The analysis presented in this note improves on that reported in [10] by using a larger data set, including the dilepton decay channel, and employing enhanced analysis techniques.

The angular distribution  $\omega$  of the down-type decay products of the  $W$  boson (charged lepton or  $d, s$  quark) in the rest frame of the  $W$  boson can be described by introducing the decay angle  $\theta^*$  of the down-type particle with respect to the top quark direction [1]:

$$\omega(\cos \theta^*) = \frac{3}{4}(1 - \cos^2 \theta^*)f_0 + \frac{3}{8}(1 - \cos \theta^*)^2 f_- + \frac{3}{8}(1 + \cos \theta^*)^2 f_+ . \quad (2)$$

Due to backgrounds and reconstruction effects, the distribution of  $\cos \theta^*$  we observe differs from  $\omega(\cos \theta^*)$ .

However, the shape of the measured  $\cos \theta^*$  distribution depends on  $f_+$  and this dependence can be used to measure  $f_+$ . We do this by selecting a data sample enriched in  $t\bar{t}$  events, reconstructing the four vectors of the two top quarks and their decay products, and then calculating  $\cos \theta^*$ . This distribution in  $\cos \theta^*$  is compared with templates for different  $f_+$  values using a binned maximum likelihood method. In the lepton plus jets channel, the kinematic reconstruction is done with a fit that constrains the  $W$  boson mass to its measured value and the top quark mass to 175 GeV/ $c$ , while in the dilepton channel the kinematics are solved algebraically with the top mass fixed to 175 GeV/ $c$ .

The DØ detector [11] comprises three main systems: the central-tracking system, the calorimeters, and the muon system. The central-tracking system is located within a 2 T solenoidal magnet. The next layer of detection involves three liquid-argon/uranium calorimeters: a central section (CC) covering pseudorapidities [12]  $|\eta| \lesssim 1$ , and two end calorimeters (EC) extending coverage to  $|\eta| \approx 4$ , all housed in separate cryostats. The muon system is located beyond the calorimetry, and consists of a layer of tracking detectors and scintillation trigger counters before 1.8 T toroids, followed by two additional similar layers after the toroids.

This measurement uses a data sample recorded by the DØ experiment and corresponds to an integrated luminosity of about  $370 \text{ pb}^{-1}$  of  $p\bar{p}$  collisions at  $\sqrt{s} = 1.96$  TeV. The data sample consists of  $t\bar{t}$  candidate events from the lepton+jets decay channel where one of the  $W$  bosons from  $t$  or  $\bar{t}$  decays into an electron or muon and a corresponding neutrino and the other  $W$  boson decays hadronically, and the dilepton channel where both  $W$  bosons decay leptonically. The lepton+jets final state is characterized by one charged lepton (e or  $\mu$ ), at least four jets (two of which are  $b$  jets), and significant missing transverse energy ( $\cancel{E}_T$ ). The dilepton final state is characterized by two charged leptons of opposite sign, at least two jets, and significant  $\cancel{E}_T$ .

We simulate  $t\bar{t}$  signal events for different values of  $f_+$  with the ALPGEN Monte Carlo (MC) program [13] for the parton-level process (leading order) and PYTHIA [14] for the subsequent hadronization. The mass of the top quark is set to  $m_t = 175$  GeV. As the interference term between  $V - A$  and  $V + A$  is suppressed by the small mass of the  $b$  quark and is therefore negligible [15], samples with  $f_+ = 0.00$  and  $f_+ = 0.30$  can be used to create  $\cos \theta^*$  templates for any  $f_+$  value by a linear interpolation of the templates. In the lepton+jets channels, we use MC samples with seven  $f_+$  values evenly spaced from 0.00 to 0.30. All seven templates from these samples are normalized to unit area and a linear fit to the contents of each  $\cos \theta^*$  bin as a function of  $f_+$  is performed. This procedure effectively averages over statistical fluctuations in the generated MC samples, thus providing a more precise model of the  $\cos \theta^*$  distribution.

The MC samples used to model background events with real leptons are also generated with ALPGEN.

Backgrounds in the lepton+jets channel arise predominantly from  $W$ +jets production, and multijet production where one of the jets is misidentified as a lepton and spurious  $\cancel{E}_T$  appears due to mismeasurement of the transverse energy in the event.

The lepton+jets event selection [16] requires an isolated lepton ( $e$  or  $\mu$ ) with transverse momentum  $p_T > 15$  GeV, no other lepton with  $p_T > 15$  GeV in the event,  $\cancel{E}_T > 20$  GeV, and at least four jets. Leptons are categorized in two classes, “loose” and “tight,” the latter being a subset of the first. Loose electrons are required to have  $|\eta| < 1.1$  and are identified by their energy deposition and isolation in the calorimeter, their transverse and longitudinal shower shapes, and information from the tracking system. For tight identification, a discriminant combining the above information must be consistent with the expectations for a high- $p_T$  isolated electron. Loose muons are identified using the information from the muon and the tracking systems. They are required to have  $|\eta| < 2.0$  and to be isolated from jets. Tight muons must also pass stricter isolation requirements based on the energy of calorimeter clusters and tracks around the muon. Only tight leptons are used in the final event selection. Jets are required to have rapidity  $|y^j| < 2.5$  and  $p_T > 20$  GeV.

To determine the number of multijet background events, we compare the number of events selected with the loose lepton criteria  $N_\ell$  with the number selected with the tight lepton criteria  $N_t$ .

The relative selection efficiency between the loose and the tight lepton criteria is different for true leptons ( $\epsilon_\ell$ ) and jets faking an isolated lepton ( $\epsilon_j$ ). We use these efficiencies, known from data control samples [16], to estimate the number of multijet background events:  $N^m = (\epsilon_\ell N_\ell - N_t)/(\epsilon_\ell - \epsilon_j)$ . We calculate  $N^m$  for each bin in the  $\cos\theta^*$  distribution from the data sample to obtain the shape of the multijet  $\cos\theta^*$  templates.

To discriminate between  $t\bar{t}$  pair production and background, a discriminant  $\mathcal{D}$  is built using input variables which exploit differences in kinematics and jet flavor. The kinematic variables used are:  $H_T$  (defined as the scalar sum of the jet  $p_T$  values), the minimum dijet mass of the jet pairs  $m_{jj\min}$ , the  $\chi^2$  from the kinematic fit, the centrality  $\mathcal{C}$  (defined as  $H_T/H_E$  where  $H_E$  is the sum of the jet energies),  $K'_{T\min}$  (defined as the distance in  $\eta - \phi$  space, where  $\phi$  is the azimuthal angle, between the closest pair of jets multiplied by the  $p_T$  of the lowest- $p_T$  jet in the pair and divided by the transverse energy of the reconstructed  $W$  boson), and aplanarity  $\mathcal{A}$  and sphericity  $\mathcal{S}$  (calculated from the four leading jets and the lepton). The last two variables characterize the event shape and are defined, for example, in Ref. [17]. Only the four leading jets in  $p_T$  are considered in computing these variables to reduce the dependence on systematic effects from the modeling of soft radiation and underlying event processes.

We utilize the fact that background jets arise mostly from light quark or gluons while two jets in  $t\bar{t}$  events arise from  $b$  quarks by considering the impact parameters of all tracks within the jet cone with respect to the primary vertex. Based on these values, we calculate the probability  $P_{PV}$  for each jet to originate from the primary vertex. We then average the two lowest  $P_{PV}$  values to form a continuous variable  $\langle P_{PV} \rangle$  that tends to be small for  $t\bar{t}$  events and large for backgrounds. This approach results in similar background discrimination but better efficiency than the traditional method of “tagging”  $b$  jets in the event.

The discriminant is built separately for the  $e+$  jets and  $\mu+$  jets channels, using the method described in Refs. [16, 18]. The distributions of signal ( $S$ ) and background ( $B$ ) events in each of the above variables are normalized to unity. For each variable  $v_i$  we fit a polynomial to the logarithm of  $S/B$  as a function of  $v_i$ . The discriminant is defined as:

$$\mathcal{D}(v_1, v_2, \dots) = \frac{\exp\left(\sum_i [\ln(S(v_i)/B(v_i))]_{\text{fit}}^i\right)}{\exp\left(\sum_i [\ln(S(v_i)/B(v_i))]_{\text{fit}}^i\right) + 1} . \quad (3)$$

We consider all possible combinations of the above variables for use in the discriminant, and all possible requirements we could place on the  $\mathcal{D}$  value, and choose the variables and  $\mathcal{D}$  criterion that gives the best expected  $N_S/\sqrt{N_S + N_B}$ , where  $N_S$  is the expected signal yield and  $N_B$  the expected background. In the  $e$  plus jets channel  $\mathcal{S}$ ,  $H_T$ ,  $K'_{T\min}$ ,  $\langle P_{PV} \rangle$ , and  $\chi^2$  are used, and  $\mathcal{D}$  is required to be  $> 0.35$ . In the  $\mu$  plus jets channel,  $\mathcal{A}$ ,  $\mathcal{C}$ ,  $m_{jj\min}$ ,  $\langle P_{PV} \rangle$ , and  $\chi^2$  are used, and  $\mathcal{D}$  is required to be  $> 0.70$ .

We then perform a binned maximum likelihood fit to compare the observed  $\mathcal{D}$  distribution in the data (shown in Fig. 1) to the sum of the distributions expected from  $t\bar{t}$ ,  $W$ +jets, and multijet events. The number of multijet events is constrained to a Poisson distribution with mean  $N^m$ . The likelihood is then maximized with respect to the number of  $t\bar{t}$ ,  $W$ +jets, and multijet events. We multiply these numbers by the efficiency for each type of event to pass the  $\mathcal{D}$  selection to determine the composition of the sample used for measuring  $\cos\theta^*$ .

In the dilepton channel, backgrounds arise from processes such as  $WW$  plus jets or  $Z$  plus jets, with  $Z \rightarrow \ell^+\ell^-$  or  $\tau\tau$ . These processes are either rare or require false  $\cancel{E}_T$  to arise from mismeasurement of jet and lepton energy, allowing a good  $S/B$  ratio to be attained using only kinematic selection criteria. The selection is detailed in [19]. Events are required to have two leptons with opposite charge and  $p_T > 15$  GeV/ $c$  and two or more jets with  $p_T > 20$  GeV/ $c$  and  $|y| < 2.5$ . Additional criteria are applied in the  $ee$  and  $\mu\mu$  channels to suppress  $Z \rightarrow \ell\ell$ , and in the  $e\mu$  channel the sum of the two leading jet  $p_T$ s and the lepton  $p_T$  must be greater than 140 GeV/ $c$ . We place a more stringent requirement on electron identification than is used in [19].

Table I lists the composition of each sample as well as the number of observed events in the data. We observe a large disparity between the number of  $t\bar{t}$  events in the  $e$ +jets channel and  $\mu$ +jets channel. The statistical significance of this effect is slightly above  $2\sigma$  (3%).

The top quark and the  $W$  boson four-momenta in the selected lepton+jets events are reconstructed using a kinematic fit which is subject to the following constraints: two jets must form the invariant mass of the  $W$  boson, the lepton and the  $\cancel{E}_T$  together with the neutrino  $p_z$  component must form the invariant mass of the  $W$  boson, and the masses of the two reconstructed top quarks

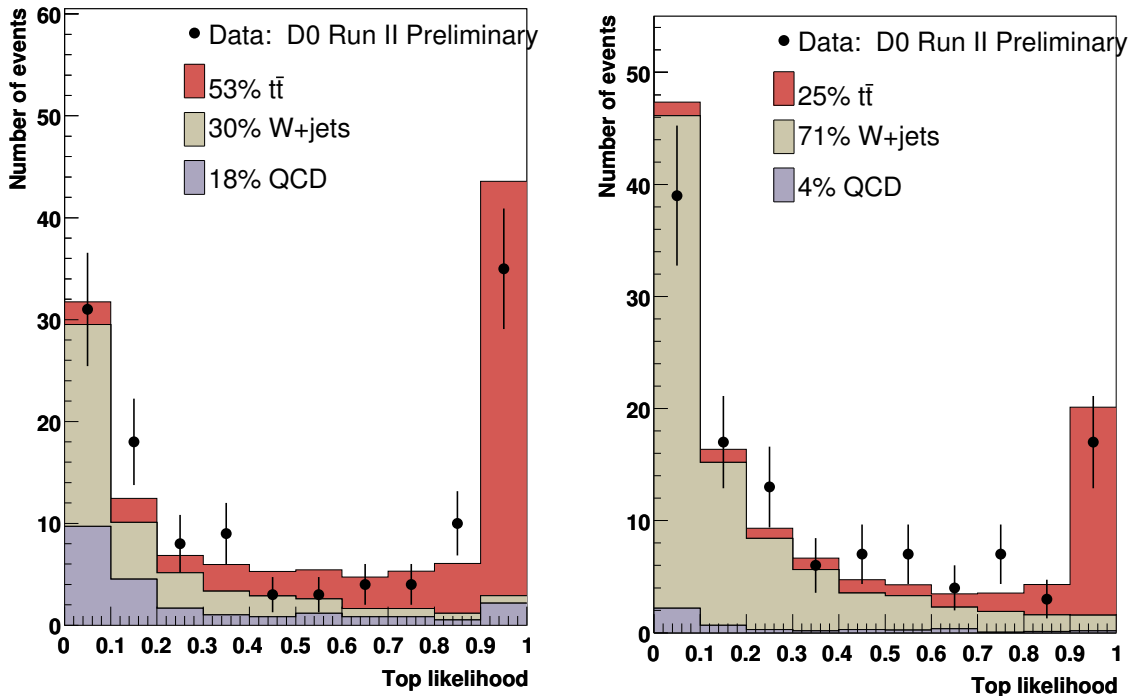


FIG. 1: Distribution of  $L_t$  for the  $e$ +jets (left) and  $\mu$ +jets (right) channels.

TABLE I: Number of events observed in each  $t\bar{t}$  decay channel, and the background level as determined by a fit to the  $\mathcal{D}$  distribution in the lepton+jets channels and the expectation from the background production rate and selection efficiency in the dilepton channels.

|                     | Observed | Background     |
|---------------------|----------|----------------|
| $e + \text{jets}$   | 64       | $13.9 \pm 7.4$ |
| $\mu + \text{jets}$ | 27       | $5.0 \pm 0.7$  |
| $e\mu$              | 15       | $2.2 \pm 0.6$  |
| $ee$                | 4        | $0.8 \pm 0.2$  |
| $\mu\mu$            | 1        | $0.4 \pm 0.1$  |

must be 175 GeV. The  $p_z$  component of the neutrino is reconstructed by exploiting the fact that the two top quark masses are equal, which gives rise to a quadratic equation for  $p_z$  [18]. In the case where the two  $p_z$  solutions lead to different results of the kinematic fit, the one with the lower  $\chi^2$  (of the fit) is kept. Among the twelve possible jet combinations, the solution with the minimal  $\chi^2$  from the kinematic fit is chosen; Monte Carlo studies show this yields the correct solution in about 60% of all cases.

The presence of two neutrinos in the dilepton final state makes the system kinematically underconstrained. However, if a top quark mass is assumed, the kinematics can be solved algebraically with a four-fold ambiguity in addition to the two-fold ambiguity in pairing jets with leptons. For each lepton, we calculate the value of  $\cos\theta^*$  resulting from each solution with each of the two leading jets associated with the lepton. To account for detector resolution we repeat the above procedure 100 times, fluctuating the jet and lepton energies within their resolutions for each iteration. The average of these values is taken as the  $\cos\theta^*$  for that lepton. This results in two  $\cos\theta^*$  measurements per event in the dilepton channels. The  $\cos\theta^*$  distribution obtained in data after the full selection and compared to standard and a  $V + A$  model expectations is shown in Figs. 2 and 3.

A binned maximum likelihood fit of signal and background  $\cos\theta^*$  templates to the data was used to measure  $f_+$ . We compute the binned Poisson likelihood ( $L(f_+)$ ) of the data to be consistent with the sum of signal and background templates at each of the seven chosen  $f_+$  values. A parabola is fit to the  $-\ln[L(f_+)]$  points to determine the likelihood as a function of  $f_+$ .

Systematic uncertainties are evaluated in ensemble tests by varying the parameters (see Table II) which can affect the shape of the  $\cos\theta^*$  distributions or the relative contribution from signal and background sources. Ensembles are formed by drawing events from a model with the parameter under study varied. These are compared to the standard  $\cos\theta^*$  templates in a maximum likelihood fit. The average shift in the resulting  $f_+$  value is taken as the systematic uncertainty and is shown in Table II. The total systematic uncertainty is then taken into account in the likelihood by convoluting the latter with a Gaussian with a width

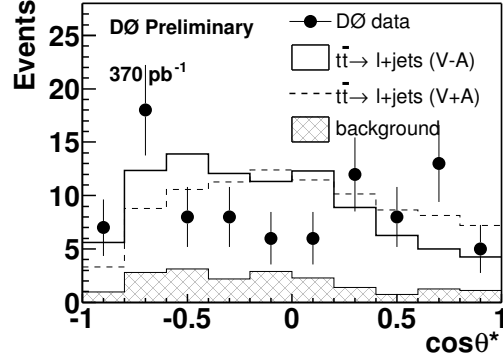


FIG. 2:  $\cos \theta^*$  distribution observed in lepton+jets events. The standard model prediction is shown as the solid line, while a model with a pure  $V + A$  interaction would result in the distribution given by the dashed line.

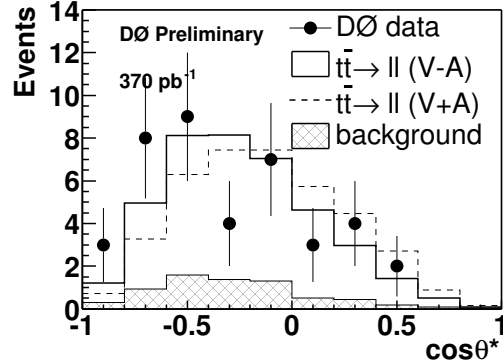


FIG. 3:  $\cos \theta^*$  distribution observed in dilepton events. The standard model prediction is shown as the solid line, while a model with a pure  $V + A$  interaction would result in the distribution given by the dashed line.

that corresponds to the total systematic uncertainty.

The dominant uncertainties arise from the uncertainties on the top quark mass and on the jet energy scale (JES). The mass of the top quark has been varied by  $\pm 5$  GeV with respect to  $m_t = 175$  GeV and the JES by  $\pm 1\sigma$  around the nominal value.

The statistical uncertainty on the  $\cos \theta^*$  templates has been taken as a systematic uncertainty. It is estimated by fluctuating them according to their statistical uncertainty.

The effect of gluon radiation in the modeling of  $t\bar{t}$  events has been studied by generating  $t\bar{t}$ +jets Monte Carlo events with the ALPGEN generator and mixing them according to the ratio of the leading order cross sections for these two processes. Effects of the chosen factorization scale  $Q$  in the generation of the  $W$ +jets events have been evaluated by using a sample generated with a different choice of  $Q$ .

The difference found between the input  $f_+$  value and the reconstructed  $f_+$  value in ensemble tests is taken as systematic uncertainty on the calibration of the analysis.

The result of the maximum likelihood fit to the  $\cos \theta^*$  distribution observed in the data is shown in Figs. 4(a) and (b) for the  $\ell$ + jets and dilepton samples, respectively. The combination is shown in Fig. 4(c).

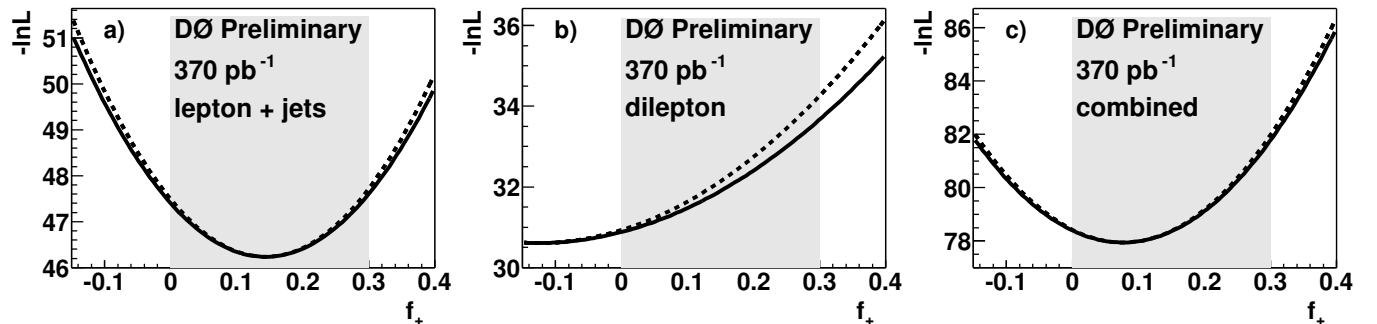


FIG. 4:  $-\ln L$  curve obtained in the a) lepton+jets channel, b) dilepton channel, and c) lepton+jets and dilepton channels combined. The dashed line includes only the statistical uncertainty while the solid line also includes the systematic uncertainties.

TABLE II: Systematic uncertainties on  $f_+$  for the two channels and for the combination.

| Source              | lepton+jets | dilepton | Combined |
|---------------------|-------------|----------|----------|
| Jet energy scale    | 0.023       | 0.039    | 0.027    |
| Top quark mass      | 0.033       | 0.070    | 0.042    |
| Template statistics | 0.030       | 0.024    | 0.024    |
| $t\bar{t}$ model    | 0.010       | 0.018    | 0.012    |
| Background model    | 0.014       | 0.007    | 0.011    |
| Calibration         | 0.010       | 0.010    | 0.008    |
| Total               | 0.054       | 0.087    | 0.058    |

The systematic uncertainties are assumed to be fully correlated except for the systematic due to the calibration of the individual analyses which is completely uncorrelated and the Monte Carlo model systematic which is partially correlated. Assuming a fixed value of 0.7 for  $f_0$ , we find

$$f_+ = 0.14 \pm 0.09(\text{stat}) \pm 0.05(\text{syst}) \quad (4)$$

using  $\ell+$  jets events, and

$$f_+ = -0.12 \pm 0.16(\text{stat}) \pm 0.09(\text{syst}) \quad (5)$$

using dilepton events. Combination of these results yields

$$f_+ = 0.08 \pm 0.08(\text{stat}) \pm 0.06(\text{syst}). \quad (6)$$

We also calculate a Bayesian confidence interval (using a flat prior distribution which is non-zero only in the physically allowed region of  $f_+ = 0.0 - 0.3$ ) which yields

$$f_+ < 0.24 @ 95\% \text{ C.L.} \quad (7)$$

As seen in Fig. 2, there is a deficit of  $\ell+$  jets data events in the central region of  $\cos(\theta^*)$ . We estimate the significance of this effect by performing a likelihood ratio test to evaluate the goodness-of-fit for the best-fit model, and find that the probability of obtaining a worse fit is 2.1%. We also evaluate the goodness of fit for the standard model hypothesis, and find a fit probability of 1.2% (statistical).

In summary, we have measured the  $W$  boson helicity in  $t\bar{t}$  decays in the lepton+jets channel. Our measurement is consistent with the standard model prediction of  $f_+ = 3.6 \times 10^{-4}$  [3]. Although the  $\ell+$  jets data does not fit well to any linear combination of  $V - A$  and  $V + A$  models, the discrepancy is not statistically significant. Analysis of the additional  $500\text{pb}^{-1}$  of data now available will clarify whether this is a fluctuation or the first hint of an interesting effect.

We thank the staffs at Fermilab and collaborating institutions, and acknowledge support from the DOE and NSF (USA); CEA and CNRS/IN2P3 (France); FASI, Rosatom and RFBR (Russia); CAPES, CNPq, FAPERJ, FAPESP and FUNDUNESP (Brazil); DAE and DST (India); Colciencias (Colombia); CONACyT (Mexico); KRF (Korea); CONICET and UBACyT (Argentina); FOM (The Netherlands); PPARC (United Kingdom); MSMT (Czech Republic); CRC Program, CFI, NSERC and WestGrid Project (Canada); BMBF and DFG (Germany); SFI (Ireland); Research Corporation, Alexander von Humboldt Foundation, and the Marie Curie Fellowships.

- 
- [1] G. L. Kane, G. A. Ladinsky, and C.-P. Yuan, Phys. Rev. D **45**, 124 (1992); R. H. Dalitz and G. R. Goldstein, *ibid.*, 1531; C. A. Nelson *et al.*, Phys. Rev. D **56**, 5928 (1997).  
[2] Review of Particle Physics, S. Eidelman *et al.*, Phys. Lett. B **592**, 1 (2004).  
[3] M. Fischer *et al.*, Phys. Rev. D **63**, 031501(R) (2001).  
[4] M. Beg *et al.*, Phys. Rev. Lett. **38**, 1252 (1977); S. H. Nam, Phys. Rev. D **66**, 055008 (2002).  
[5] K. Fujikawa and A. Yamada, Phys. Rev. D **49**, 5890 (1994); P. Cho and M. Misiak, Phys. Rev. D **49**, 5894 (1994); C. Jessop, SLAC-PUB-9610.  
[6] CDF Collaboration, T. Affolder *et al.*, Phys. Rev. Lett. **84**, 216 (2000).  
[7] DØ Collaboration, V. M. Abazov *et al.*, Phys. Lett. B **617**, 1 (2005).  
[8] CDF Collaboration, D. Acosta *et al.*, Phys. Rev. D **71**, 031101 (2005).  
[9] CDF Collaboration, A. Abulencia *et al.*, submitted to Phys. Rev. Lett.  
[10] DØ Collaboration, V. M. Abazov *et al.*, Phys. Rev. D **72**, 011104(R) (2005).

- [11] DØ Collaboration, V. M. Abazov *et al.*, “The Upgraded DØ detector,” submitted to Nucl. Instrum. Methods Phys. Res. A.
- [12] Rapidity  $y$  and pseudorapidity  $\eta$  are defined as functions of the polar angle  $\theta$  with respect to the proton beam and the parameter  $\beta$  as  $y(\theta, \beta) \equiv \frac{1}{2} \ln[(1 + \beta \cos \theta)/(1 - \beta \cos \theta)]$  and  $\eta(\theta) \equiv y(\theta, 1)$ , where  $\beta$  is the ratio of a particle’s momentum to its energy.
- [13] M. L. Mangano *et al.*, JHEP **07**, 001 (2003).
- [14] T. Sjöstrand *et al.*, Comp. Phys. Commun. **135**, 238 (2001).
- [15] J. G. Körner, private communication.
- [16] DØ Collaboration, V. M. Abazov *et al.*, hep-ex/0504043.
- [17] V. Barger *et al.*, Phys. Rev. D **48**, R3953 (1993).
- [18] DØ Collaboration, B. Abbott *et al.*, Phys. Rev. D **58**, 052001 (1998).
- [19] DØ Collaboration, V. M. Abazov *et al.*, in preparation.